Combustion process optimization for oxymethylene ether fuels in a heavy-duty application

Kai Gaukel, Patrick Dworschak, Dominik Pélerin,
Martin Härtl, Georg Wachtmeister

Institute of Internal Combustion Engines
at Technical University of Munich

Introduction

Oxymethylene ethers (OME) are synthetic fuels based on C1 chemistry, which can be produced from sustainable feedstocks like waste CO_2 and hydrogen out of electrolysis [10]. The constitutional formula of OME_n is CH_3-O-$(CH_2$-O$)_n$-CH_3 while the number of oxymethylene groups n determines the chain-length of the molecule. OME_n with $0 \leq n \leq 6$ are suitable as diesel fuels because of their good ignitability. OME_0, also known as dimethyl ether, is gaseous under standard conditions and OME_1 to OME_6 are liquid under standard conditions and therefore easier to handle. However, OME_6 has a melting point at 38 °C and should be avoided in OME mixtures to avoid filter plugging [16].

Ogawa et al. [13] have already shown in early studies the significant soot reduction when using neat OME_1 instead of diesel and the possibility to use high exhaust gas recirculation (EGR) levels to reduce NO_x emissions at the same time. When reaching stoichiometric conditions, the raw emissions of THC, CO and NO_x are rising rapidly, but the emissions can be converted with a three-way catalyst.

The effect of a high EGR tolerance without increasing soot emissions was also shown by Schmitt et al. [18] and Härtl et al. [8], while in the latter OME_{1a} was identified to be the most effective oxygenate to reduce soot emissions. Kitamura et al. [11] and Sun et al. [19] explain this effect by the molecular structure of OME_n. On the other hand, it is the high oxygen content of at least 42.1 wt.-% for OME_1 and the missing C-C bonds. The latter are necessary for the formation of acetylene, which is after Frenklach [4] the primary precursor for the formation of polycyclic aromatic hydrocarbons and therefore for soot formation.

Another critical emission occurring at high EGR rates is methane, because it is hardly converted in the diesel oxidation catalyst (DOC). Methane is preferably formed due to the methyl caps of the molecule. Even when using OME_2 [5] or a mixture of $OME_{3\text{-}6}$ [15], where the proportion of methyl in the molecule is smaller, there is no significant reduction in methane emissions. Pélerin et al. [15] recommend to avoid stoichiometric air/fuel equivalence ratios, because of both, emissions and efficiency. Barro et al. [1] used an 80/20 % mixture of $OME_{3/4}$ in a heavy-duty engine with enlarged injector nozzle. They showed that NO_x emissions can be reduced below the EURO VI limit of 0.4 g/kWh when approaching globally stoichiometric conditions. However, at stoichiometric conditions the HC, CO and CH_4 emissions are rising rapidly.

Regarding indicated efficiency in OME_1 operation Münz et al. [12] and Feiling et al. [3] have shown a benefit at low to medium loads. At higher loads the rate of heat release is limited by the maximum nozzle flow rate and inhibits the combustion to finish earlier. The same effect is reported by Härtl et al. in [6] and by Pélerin et al. in [15].

Damyanov et al. [2] improve indicated efficiency by increasing rail pressure with OME_{1a} from 1000 to 1600 bar at an IMEP of 15 bar. Thus, the same injector nozzle achieves higher flow rates and indicated efficiency reaches nearly the same level as with diesel. Pélerin et al. [16] and Härtl et al. [7] use larger injector nozzle holes, which compensate the lower energy content of OME fuels and additionally allow a reduction of the rail pressure from 1800 to 1000 bar. The resulting nozzle has a 2.5 times higher volumetric nozzle flow and therefore injects the same amount of energy in the same time when using OME_{1b} as when compared to the standard configuration and diesel. This leads to an increased indicated efficiency in the whole engine-map compared to standard diesel operation. The shortened combustion rises the mean cylinder temperatures and therefore slightly increases NO_x emissions. However CO and volatile organic compounds (VOC) are reduced. Soot mass and particle number emissions are on lowest levels for both nozzles.

The latter engine configuration, with the large injector nozzle and lowered rail pressures, is the basis reference for this work. The objective is to do an optimization study of the piston bowl shape by 3D-CFD simulation for the combustion of OME_1 with the primary focus on reduced emission levels and enhanced efficiency.

Fuel properties

The investigations in this work are carried out with OME_1, which is widely available and fundamentally tested as a highly oxygenated fuel with lowest soot formation tendencies. Table 1 shows the most important values for OME_1 and OME_{1b}. The neat substance is used in the 3D-CFD simulation due to modeling simplifications and OME_{1b}, with additives, is used in the experimental investigations, mainly because of the injection system and its requirement of a better lubricity and higher viscosity. The utilization of long-chained polyether molecules as additive substances in OME_{1b} leads to slight increases in lower heating value (LHV) and density. Ignitability is also enhanced, which is represented by the cetane number of 40 instead of 29.3. The diesel equivalent describes the volumetric amount of OME_1 needed to reach the same amount of energy as with diesel fuel.

Table 1 Investigated fuels

	Unit	OME_1	OME_{1b}*
LHV	MJ/kg	22.4	22.5
Cetane number	-	29.3	40
Kin. Viscosity (measured at 20 °C)	mm²/s	0.33	0.71
HFFR Lubricity (measured at 20 °C)	µm	759	278
Density	kg/m³	0.86	0.87
Boiling point	°C	42	42
Melting point	°C	-105	-105
Oxygen content	wt.-%	42.1	42.1
Diesel equivalent	m³/m³	1.77	1.75

*OME_1 with 3 wt.-% additivation of long-chained polyether

Simulative Optimization Study

Recent experimental investigations at the Technical University of Munich [16] led to the result that adapting the injector nozzle flow improves indicated efficiency in OME_{1b} operation. An enlargement of the nozzle hole diameter from 198 µm to 313 µm, which equals a volumetric flow factor of 2.5, compensates the lowered rail pressure of 1000 bar and the LHV of OME_{1b}, so that the same energy flow as with paraffinic diesel fuel and the base nozzle at 1800 bar rail pressure is reached. Proceeding from this result, the piston shape geometry is optimized by a 3D-CFD simulation study. The focus of the optimization is on the one hand on NO_x emissions and on the other hand on indicated efficiency.

Modeling

The calculations are set up in STAR-CD as Reynolds Averaged Navier-Stokes (RANS) simulations with the k-ε RNG turbulence model, in order to keep simulation time in a reasonable extent. The moving meshes for the calculations are created with the software module es-ice.

The liquid fuel is injected as a Lagrangian phase in a Euler modeled gaseous phase. The initial conditions of the injected parcels are defined by geometrical values of the nozzle, the injection rate and an injection vector calculated by the atomization model after Huh. The Kelvin-Helmholtz Rayleigh-Taylor model is used for calculating droplet break-up. The injection rates used in this work are derived from injection rates, which are measured with Diesel and DME by the injection system supplier DENSO. For the use in the simulation, these injection rates are scaled by the density ratio between Diesel or DME and OME_1. This model set up showed the best results for the validation of the liquid

and evaporated penetration length in isolated spray calculations with OME_1. On this occasion, the VKA of the RWTH Aachen provided the optical spray measurements with an injector of the same type, but smaller nozzle holes (171 µm instead of 313 µm) for the validation.

A full-engine model, including intake and exhaust ports, is used to determine the conditions for temperature, turbulent kinetic energy and flow velocity in the cylinder, shortly after the time when the intake valves are closed. The combustion simulation of the different piston geometries is then carried out in simplified symmetric combustion chamber sector models, which represent one eighth of the whole combustion chamber including one hole of the injector. The most important simplifications are the elimination of the area around the valve seats to a flat cylinder head, the valve pockets in the piston and the injector nozzle tip. The missing volumes are added to the top land, so that the compression ratio is kept constant at $\varepsilon = 17$.

For ignition and combustion calculation, an approach with the ECFM-3Z model and tabulated ignition data is used. The ignition tables are created by the calculation of detailed chemistry models with the software module DARS, based on the detailed reaction mechanisms published by Sun [19] and He [9]. The implementation of temperature dependent thermodynamical gaseous properties is also based on the latter data. The temperature dependent properties for the liquid phase (density, surface tension, viscosity, saturation pressure, conductivity and heat of vaporization) of OME_1 are implemented after Yaws [20]. Because of the complexity of calculating a multi-component fuel, OME_1 is calculated as a neat substance, neglecting the influence of the three wt.-% additive on the fuel properties.

Operating point simulation

All of the following calculations in this work are carried out at the same operating point at an engine speed of 1200 1/min, an IMEP of 13 bar, a boost pressure of 1.95 bar, a rail pressure of 1000 bar, an injected fuel mass of 230 mg/stroke and a 313 µm nozzle hole diameter. Wall temperatures are set to 420 K on the liner, 450 K on the piston crown and 500 K on combustion dome. The fuel is injected by a pilot and main injection.

Validation Combustion

The validation of the CFD simulation results with the measurement data in Figure 1 shows a good match of the pressure and temperature levels during compression. The pilot injection ignites a little late, due to not considering the cetane number enhancing

additive. The shape of the rate of heat release matches good to the data from measurement. Whereas the overestimation of the calculated rate of heat release does not fit to the underestimated pressure and temperature levels. This leads to the assumption of uncertainties in the heat capacity of the cylinder mass, resulting from the gaseous fuel properties, because the effect only occurs as soon as fuel is injected. However, the quality of the results is good enough to derive tendencies for the piston bowl shape optimization. However, for further improvement it is planned to use detailed chemistry models based on a recently published reaction mechanism by Ren [17], which will also allow to get a better understanding of emission formation.

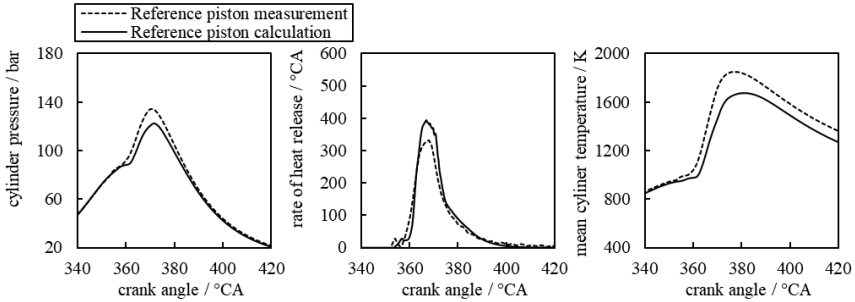

Figure 1 Comparison between combustion simulation and measurement data

Calculated piston designs

An overview of the calculated piston bowl shapes is given in Figure 2. For all piston shapes the compression ratio was kept constant at $\varepsilon = 17$. The main idea of the more narrow piston bowls V1, V5, V6, V7, V8 and V9 is to force an earlier spray break-up regarding the shorter liquid penetration depth of neat OME_1 with its high saturation pressure referred to diesel spray. Piston V2 was designed to reduce wall heat losses by leading a larger amount of the evaporated fuel in the upper region during combustion by a deeper step contour with the reason that the temperature difference between gas and cylinder head is less then to the piston. Piston V5 and V6 are a combining the variations of V1 and V2 with different step contours. Piston V7 and V8 are using deeper bowls, whereas V9 and V10 are classical ω-bowl shapes. Piston V3 and V4 were designed to minimize piston wall area.

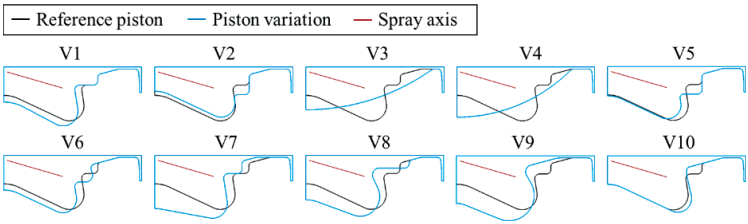

Figure 2 Calculated piston bowl shapes

Simulative Results

The simulations are assessed primarily by the piston work created from the fuel, which represents the indicated efficiency, as always the same fuel mass is injected. The second objective is the reduction of NO emissions and the third is the reduction of unburnt fuel. The overview in Figure 3 shows the results referring to the reference piston calculation. The piston designs V2-V7 lead to lower piston work and a therefore low estimated efficiency. Piston V1 also leads to slightly lower piston work and a strong increase in unburnt fuel emissions, but at lower NO emissions. Piston V10 shows no considerable benefit at all. Piston V8 slightly increases piston work at an acceptable increase of the NO level and a decrease of unburnt fuel emissions of 44 %. Piston V9 shows lowered NO and unburnt fuel emissions at a comparable efficiency. For these reasons piston V8 and V9 are manufactured and prepared for experimental evaluation.

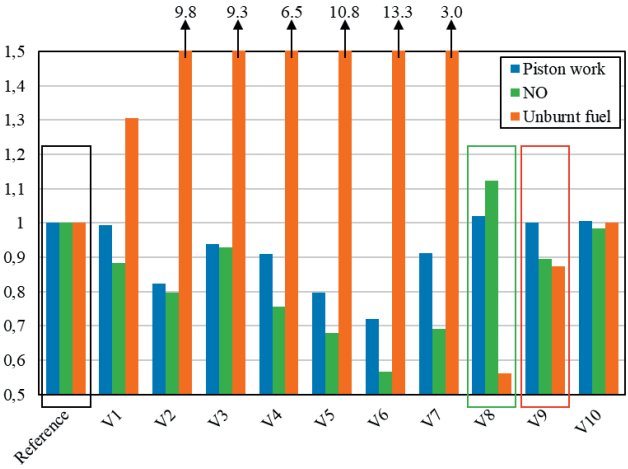

Figure 3 CFD calculation result overview for the different piston bowl shapes

Experimental Investigations

Experimental setup

The single cylinder engine for the experimental investigations is derived from the MAN D20 series. Its displacement of 1.753 dm³ results from a bore of 120 mm and a stroke of 155 mm. The reference piston has a step bowl shape and a geometrical compression ratio of ε = 17. The high pressure fuel system is supplied by DENSO, while an G4S injector with optimized eight-hole nozzle, each with a hole diameter of 313 µm and resulting 5075 cm³/min volumetric flow rate, is used. To avoid boiling of OME_{1b} in the control volume of the injector and the fuel return line, the counter pressure is set to 25 bar by an overflow valve. The intake air is conditioned and charged externally. To represent real engine conditions the turbocharger is replaced by an exhaust throttle which controls the exhaust backpressure according to the series engine-map, to reach a turbocharger efficiency of η_{TC} = 60 %. Exhaust gas is fed back to the intake through a cooler while an EGR throttle valve controls the amount of recirculated gas. A DOC is used for the exhaust gas aftertreatment. The DOC has a volume of 1.64 dm³, a 40 g/ft³ platinum coating and a 300/600 LS carrier from Continental Emitec GmbH. The sampling position for the exhaust gas measurement system AVL Sesam i60 FT Series II can be switched before and behind the DOC. This system consists of a FTIR for measuring volatile compounds, which is particularly set up to measure unburnt OME_1 concentration and further products of incomplete combustion like formaldehyde or methane. The FID is used to measure the summed up amount of VOC and the PMD for the oxygen content of the exhaust gas. The EGR rate is determined by a CO_2 concentration measurement with an IRD in the intake system. An AVL 483 Microsoot Sensor is used for soot mass measurement after a photoacoustic principle and a Horiba MEXA-2300 SPCS is used to determine particle number concentration according to the particle measurement program with a condensation particle counter with a cut-off at 50 % at 23 nm particle size.

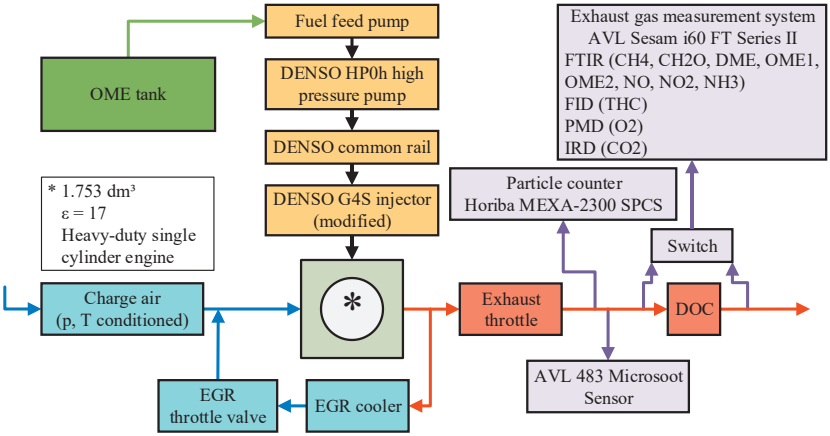

Figure 4 Testbench setup

Test design

The piston designs Reference, V8 and V9 are examined in an EGR sweep at the optimized operating point of the simulation and four additional operating points (OP1-4) listed in Table 2. Each of the additional OP is measured without EGR and with an EGR level so that $\lambda = 1.25$ is reached. NO_x emission levels around the EURO VI requirements of 0.4 g/kWh were achieved for this EGR level in the EGR sweep. OP1-OP4 are chosen to show the influence of different engine speed and load levels. The boost pressures equal the series engine-map application. Rail pressure is set to 1000 bar as the injector nozzle is designed to use lower rail pressures. The center of combustion is controlled by injection timing to be at 8 °CA after top dead center (TDC) with a pilot and main injection strategy. The start of pilot injection is set to 5 °CA before the begin of the main injection with an energizing duration of 0.25 ms. The intake air is conditioned to 40 °C and OME_{1b} is used as fuel for all operating points. To reduce statistical impact each operating point is measured twice.

Table 2 Test design

	Unit	EGR Variation	OP1		OP2		OP3		OP4	
IMEP	bar	13	10		10		15		15	
Engine speed	1/min	1200	1000		1250		1250		1500	
EGR	wt.-%	0-25	0	23	0	20	0	20	0	28
$\lambda_{Brettschneider}$	-	max - 1.0	max	1.25	max	1.25	max	1.25	max	1.25
Boost pressure	bar	1.94	1.54		1.55		2.28		2.38	
Rail pressure	bar	1000	1000		1000		1000		1000	
Air temperature	°C	40								
Center of comb.	°CA a. TDC	8								
Exhaust back-pressure		η_{TC} = 60 %								
Injection strategy		Pilot and main injection								
Fuel		OME_{1b}								

Experimental results

The results in Figure 5 give an overview of the emission characteristics and the indicated efficiency for the EGR sweep at the same operating point that the piston design is optimized for. All pistons lead to a comparable efficiency without EGR, with V8 it is slightly improved and with V9 it is nearly equal, as predicted by simulation. Using piston V9 reduces NO_x emissions from 14.2 g/kWh with the reference piston down to 9.9 g/kWh. However, in contrast to the simulation, using piston V8 also reduces NO_x down to 11.7 g/kWh at a slightly improved indicated efficiency. With increasing EGR the efficiency for piston V9 decreases earlier as with the other two pistons. The missing step in the ω-bowl shape leads to a worsened mixture formation during the diffusive combustion. This results in more products of incomplete combustion like VOC and CO. The larger volume above the bowl step can explain the slightly stronger increase in CO emissions for piston V8. The injection mainly directs in the piston bowl and thus less oxygen takes part in the combustion. Additionally due to the high EGR rates, the oxygen distribution is too low for a complete combustion. At $\lambda = 1.25$ even the benefit in NO_x emissions vanishes with the optimized geometries, as there is enough EGR in the cylinder to reduce combustion temperatures also with the reference piston and a further increase of EGR only has a small effect on the NO_x emissions. At $\lambda = 1.15$ methane emissions are starting to rise for all pistons. This shows that the main part of the VOC

emissions consists of methane. No considerable soot emissions are measured, even under stoichiometric conditions. Particle number measurements are for all pistons in the same low order of magnitude, with a benefit of around 1.5E+11 #/kWh for the optimized pistons. The missing C-C bonds in the fuel, which are necessary for acetylene formation, explain the effect on the particulates for OME combustion on the one hand and on the other hand the high oxygen content avoids fuel rich areas during combustion.

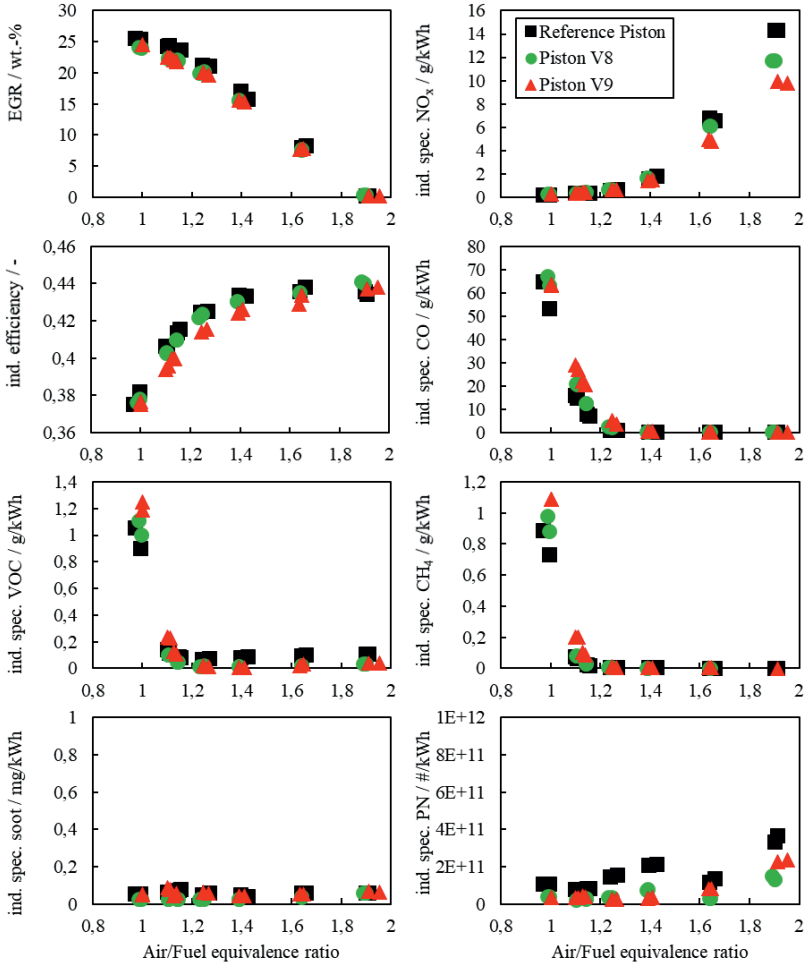

Figure 5 Emission and efficiency results EGR sweep at IMEP = 13 bar and n = 1200 1/min

The combustion characterization in Figure 6 shows the normalized heat release and mean cylinder temperature. The earlier start of combustion with piston V8 is explained by the earlier injection timing to keep the center of combustion at 8 °CA after TDC. This is necessary because the rate of heat release after the center of combustion begins to decelerate. This effect keeps the mean cylinder temperature lower with the result of reduced NO_x emissions. The rate of heat release with piston V8 is also lower as with the reference piston leading to lower temperatures and therefore a reduction of NO_x emissions. The exhaust gas temperature with about 414 °C is the same for all pistons. The lowered mean cylinder temperatures reduce wall heat losses, which explains the slightly improved efficiency. During the combustion at $\lambda = 1.25$ the mean cylinder temperature with the reference piston is comparable to the other pistons and so it is confirmed why the NO_x benefit with the optimized pistons is less distinct at this operating point. The total heat release shows concurrently, that combustion with the optimized pistons gets more incomplete as with the reference piston, what explains the increasing CO and VOC emissions, especially for piston V9.

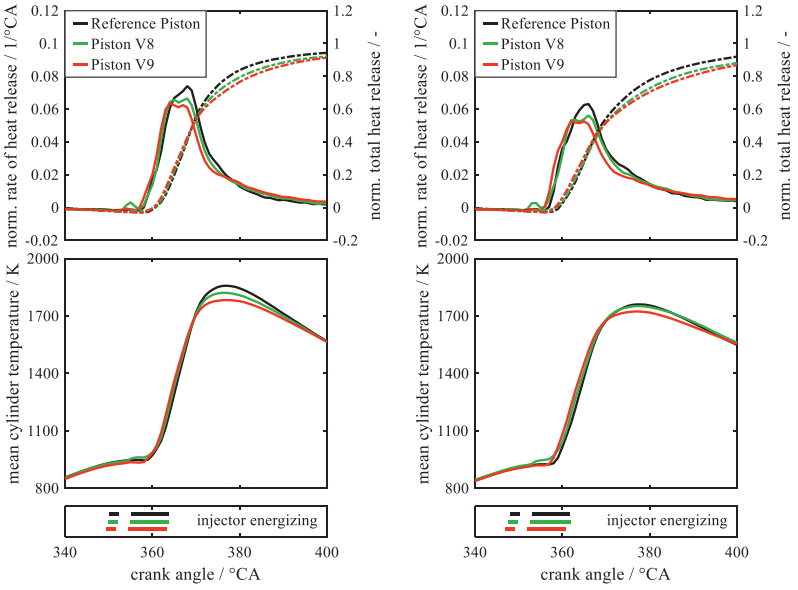

Figure 6 Combustion behavior at IMEP = 13 bar, n = 1200 1/min, no EGR (left) / $\lambda = 1.25$ (right)

The results in Figure 8 are verifying the tendencies of the EGR sweep under different load and engine speed conditions. Hereby at OP1 with piston V8 and without EGR, the

EGR valve did not close properly and from that, an EGR rate of 2.5 wt.-% arises. This influence can be neglected on the shown results, except on NO_x emissions, which are a little too low. At OP1 with the reference piston geometry the FID did not work properly, so that the VOC emissions are not measured correctly and for that reason they are not shown here. However, the methane emissions give a good estimation for the VOC.

The optimized pistons lead to reduced NO_x emissions together with acceptable indicated efficiency at the operating points without EGR. At an IMEP of 15 bar the NO_x benefit with piston V8 is getting smaller as at the 10 bar operating points. NO_x is rising with increasing load and the resulting higher combustion temperatures and NO_x emissions are getting lower with increasing engine speed. This is verified with all pistons. A loss in efficiency by adding high EGR rates is less distinct at lower engine speed, except for piston V9. The increase of VOC and CO at $\lambda = 1.25$ is evident at all operating points, but less distinct at higher loads. Piston V9 even eliminates the methane emissions to negligible levels at an IMEP of 15 bar. In the other operating points piston V9 shows incomplete combustion behavior and therefore low efficiency. The slightly higher exhaust gas temperatures with piston V9 and EGR confirm the assumption of a slow incomplete combustion. With piston V8, the CO levels at $\lambda = 1.25$ are comparable to those with the reference piston, except at OP4. This proves the assumption of a lack of oxygen in the piston bowl area where the combustion occurs, because the effect gets worse with higher injected fuel mass and higher piston velocities. A larger part of the fuel mixture stays in the piston bowl area as the piston moves down and there the diffusive combustion takes place. Thus, the oxygen stored in the upper part of the combustion chamber participates less in combustion. The calculation result in Figure 7 exemplarily shows the shift of the combustion into the bowl area, at the operating point of the bowl shape optimization. The soot mass levels are negligible under all investigated conditions. Particle numbers are very low throughout all measured operating points, but the narrower bowl shapes lead to an additional decrease of particle numbers in most of the operating points.

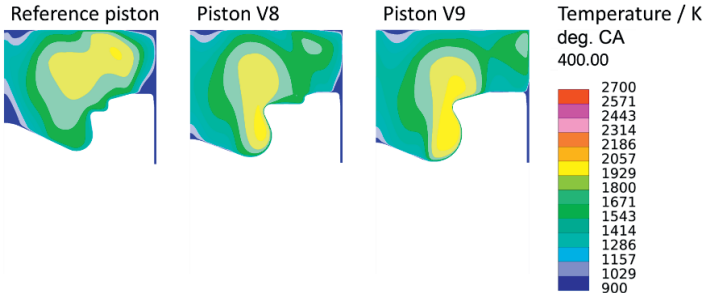

Figure 7 Temperature distribution from CFD at IMEP = 13 bar, n = 1200 1/min, no EGR

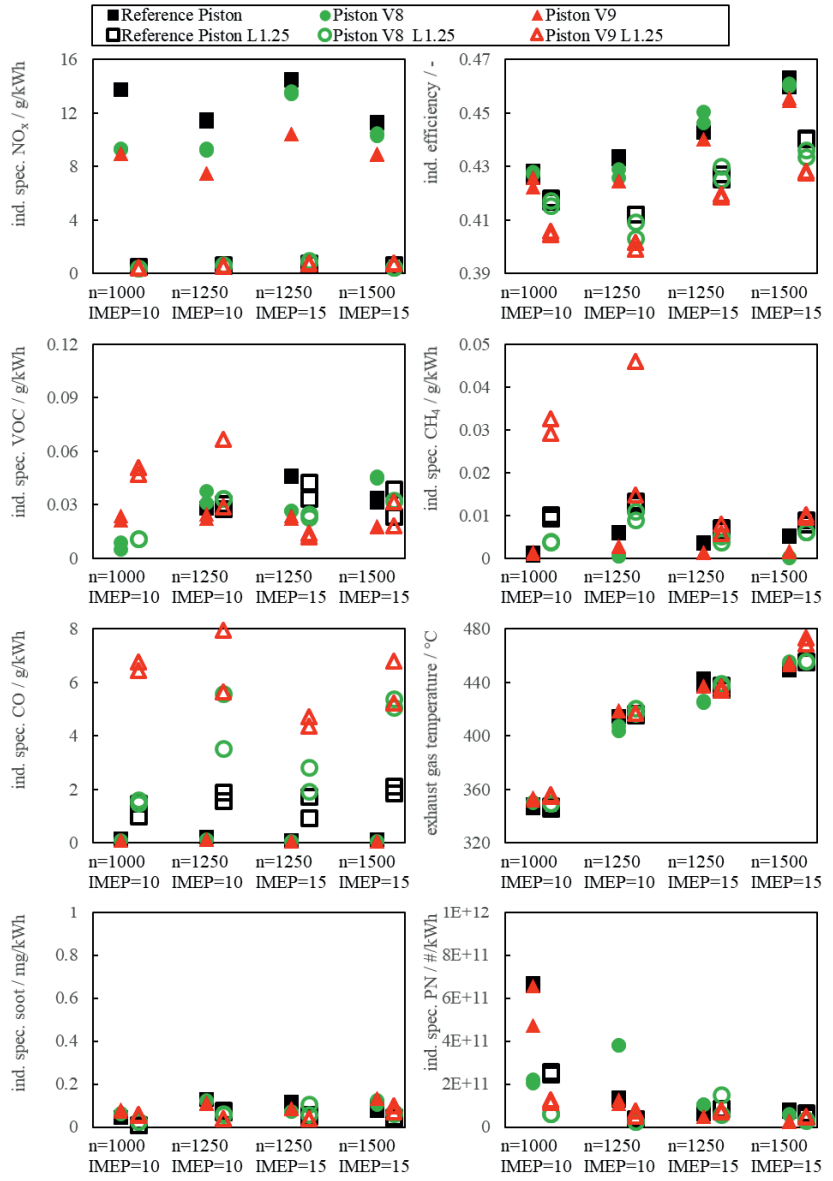

Figure 8 Comparison of emissions and efficiency at different operating points

Conclusion and Outlook

The simulative investigations and the validation with the experiments have shown, that tendencies of different geometry shapes on the combustion behavior can be predicted and the adaption of the piston bowl shape design has a strong influence on the combustion behavior. The comparison between ω-bowl and step bowl shape has shown, that a good mixture formation is necessary, especially for high EGR rates. The combustion becomes incomplete and inefficient. There is still no significant soot formation detectable, but the VOC and CO emissions are rising. This means a step bowl piston should be preferred for the use of OME_{1b}, as the step improves the mixture formation.

The narrower bowl shapes lead to a good efficiency at lowered NO_x levels, as long as there is globally enough oxygen in the combustion chamber. If the EGR rate is too high, combustion becomes incomplete again. Further simulative investigations should be done to optimize the combustion behavior under high EGR conditions and so avoid the incomplete combustion for a narrow bowl. For example, a variation of the bowl pin height and the corresponding angle in the bowl shape or a variation of the spray axis direction would be conceivable to improve the mixture formation.

Acknowledgement

The published investigations have been carried out during the research project “xME-Diesel” which is funded by the German Federal Ministry for Economic Affairs and Energy. The authors express their gratitude to Analytik Service GmbH, INEOS Paraform GmbH, Dow Europe GmbH, Sasol Germany GmbH, Continental Emitec GmbH for the supply with fuel components and catalysts and additionally to all project partners for their collaboration.

References

[1] C. Barro, M. Parravicini, K. Boulouchos, A. Liati, “Neat polyoxymethylene dimethyl ether in a diesel engine; part 2: Exhaust emission analysis”, Fuel 234, pp.1414-1421, 2018.

[2] A. Damyanov, P. Hofmann, J. Drack, T. Pichler, N. Schwaiger, M. Siebenhofer, „Operation of a Diesel Engine with Biogenous Oxymethylene Ethers“, 26th Aachen Colloquium Automobile and Engine Technology 2017, pp. 289-314.

[3] A. Feiling, M. Münz, C. Beidl, “Potential of the Synthetic Fuel OME_{1b} for the Soot-free Diesel Engine”, MTZ extra – Fuels and Lubricants of the Future, February 2016, pp. 16-21.

[4] M. Frenklach, H. Wang, “Detailed Mechanism and Modeling of Soot Particle Formation.” In Bockhorn, H. (Hrsg.) Soot Formation in Combustion, pp. 165 - 192, 1994.

[5] K. Gaukel, D. Pélerin, M. Härtl, G. Wachtmeister, J. Burger, W. Maus, E. Jacob, „The Fuel OME2: An Example to Pave the Way to Emission-Neutral Vehicles with Internal Combustion Engine”, Lenz (Hrsg.) 37. Internationales Wiener Motorensymposium, Vienna 2016, ISBN: 978-3-18-379912-1.

[6] M. Härtl, K. Gaukel, D. Pélerin, G. Wachtmeister, “Oxymethylene Ether as Potentially CO2-neutral Fuel for Clean Diesel Engines Part 1: Engine Testing”, MTZ worldwide, Vol 78, 02/2017, pp.52-58, DOI: https://doi.org/10.1007/s38313-016-0163-6.

[7] M. Härtl, D. Pélerin, P. Dworschak, T. Maier, A. Stadler, S. Blochum, K. Gaukel, E. Jacob, G. Wachtmeister, „Potential of the Sustainable C1-Fuels OME, DMC and MeFo for Particulate Free Combustion in DI and SI Engines”, Liebl J., Beidl C., Maus W. (eds) Internationaler Motorenkongress 2018. Springer Vieweg, Wiesbaden, DOI: https://doi.org/10.1007/978-3-658-21015-1_29.

[8] M. Härtl, P. Seidenspinner, E. Jacob, G. Wachtmeister, “Oxygenate screening on a heavy-duty diesel engine and emissions characteristics of highly oxygenated oxymethylene ether fuel OME1“, Fuel 153, pp. 328-335, 2015.

[9] T. He, Z. Wang, X. You, H. Liu, Y. Wang, X. Li, X. He, “A chemical kinetic mechanism for the low- and intermediate-temperature combustion of Polyoxymethylene Dimethyl Ether 3 (PODE3)”, Fuel 212, pp. 223-235, 2018.

[10] E. Jacob, W. Maus, “Oxymethylene Ether as Potentially Carbon-neutral Fuel for Clean Diesel Engines Part 2: Compliance with the Sustainability Requirement”, MTZ worldwide, Vol. 78, pp. 52-57, 2017, DOI: 10.1007/s38313-017-0002-4.

[11] T. Kitamura, T. Ito, J. Senda, H. Fujimoto, “Detailed Chemical Kinetic Modeling of Diesel Spray Combustion with Oxygenated Fuels”, SAE Technical Paper 2001-01-1262, 2001, DOI: 10.4271/2001-01-1262.

[12] M. Münz, A. Feiling, C. Beidl, M. Härtl, D. Pélerin, G. Wachtmeister, “Oxymethylene ether (OME1) as a synthetic low-emission fuel for DI diesel engines” Liebl J., Beidl C. (eds) Internationaler Motorenkongress 2016. Springer Vieweg, Wiesbaden, DOI: 10.1007/978-3-658-12918-7_41.

[13] H. Ogawa, N. Nabi, M. Minami, N. Miyamoto, K. Bong-Seock, “Ultra Low Emissions and High Performance Diesel Combustion with a Combination of High EGR, Three-Way Catalyst, and a Highly Oxygenated Fuel, Dimethoxy Methane (DMM)”, SAE 2000-01-1819.

[14] H. Ogawa, N. Miyamoto, M. Yagi: Chemical-Kinetic Analysis on PAH Formation Mechanisms of Oxygenated Fuels. SAE 2003-01-3190, 2003.

[15] D. Pélerin, K. Gaukel, M. Härtl, G. Wachtmeister, “Recent results of the sootless diesel fuel oxymethylene ether”, Liebl J., Beidl C. (eds) Internationaler Motorenkongress 2017. Springer Vieweg, Wiesbaden, DOI: 10.1007/978-3-658-17109-4_28.

[16] D. Pélerin, K. Gaukel, M. Härtl, G. Wachtmeister, „Simplifying of the Fuel Injection System and lowest Emissions with the alternative Diesel Fuel Oxymethylene Ether”, 16th Conference “The Working Process of the Internal Combustion Engine”, Graz, 2017.

[17] S. Ren, Z. Wang, B. Li, H. Liu, J. Wang, „Development of a reduced polyoxymethylene dimethyl ethers (PODEn) mechanism for engine applications”, Fuel 238, pp. 208-224, 2019.

[18] M. Schmitt, A. Feiling, C. v. Pyschow, C. Beidl, E. Jacob, „Potential des synthetischen Kraftstoffs OME1 zur Emissionsreduzierung bei Dieselbrennverfahren“, Internationaler Motorenkongress 2015, Baden-Baden, Februar 2015. Springer Vieweg, Wiesbaden, pp. 265-281, DOI 10.1007/978-3-658-08861-3_6.

[19] W. Sun et al., “Speciation and the laminar burning velocities of poly(oxymethylene) dimethyl ether 3 (POMDME3) flames: An experimental and modeling study”, Proceedings of the Combustion Institute 2016, DOI: 10.1016/j.proci.2016.05.058.

[20] C. L. Yaws, “Transport Properties of Chemicals and Hydrocarbons”, 2009, ISBN: 978-0-8155-2039-9.